Available online at www.sciencedirect.com
SCIENCE DIRECT
Journal of Magnetic Resonance 179 (2006) 323–328
JMR Journal of Magnetic Resonance
www.elsevier.com/locate/jmr

Communication

Two-dimensional Fourier transform of arbitrarily sampled NMR data sets

Krzysztof Kazimierczuk [a], Wiktor Koźmiński [a,*], Igor Zhukov [b]

[a] Department of Chemistry, Warsaw University, ul. Pasteura 1, 02-093 Warsaw, Poland
[b] Institute of Biochemistry and Biophysics, Polish Academy of Sciences, ul. Pawińskiego 5a, 02-106 Warsaw, Poland

Received 5 December 2005; revised 25 January 2006
Available online 20 February 2006

Abstract

A new procedure for Fourier transform with respect to more than one time variable simultaneously is proposed for NMR data processing. In the case of two-dimensional transform the spectrum is calculated for pairs of frequencies, instead of conventional sequence of one-dimensional transforms. Therefore, it enables one to Fourier transform arbitrarily sampled time domain and thus allows for analysis of high dimensionality spectra acquired in a short time. The proposed method is not limited to radial sampling, it requires only to fulfill the Nyquist theorem considering two or more time domains at the same time. We show the application of new approach to the 3D HNCO spectrum acquired for protein sample with radial and spiral time domain sampling.

Keywords: NMR spectroscopy; Fourier transformation; Data sampling; Proteins; Fast multidimensional data acquisition; Quaternions

1. Introduction

The multidimensional NMR spectroscopy provides unique source of information about biomolecular structure, interactions, and dynamics. The conventional way to generate N-dimensional NMR data sets with $(N-1)$ indirectly sampled time domains is to acquire a one-dimensional spectrum for each combination of equally spaced indirectly sampled evolution times. It allows consecutive application of standard one-dimensional Fourier transform (FT) [1] Eq. (1) with respect to N separate evolution times.

$$S(\omega) = \int_{-\infty}^{\infty} \mathrm{d}t f(t) \exp(-\mathrm{i}\omega t). \tag{1}$$

Assuming that each transformation requires m data points, it is necessary to acquire m^{N-1} of one-dimensional FIDs. In consequence, the time of experiment increases rapidly with number of dimensions. Therefore, the minimal possible measurement time is rather sampling than sensitivity limited [2]. In the last few years, a number of new ideas leading to the acceleration of the acquisition of multidimensional data sets have been proposed [3–6]. The new approaches involve: spatially encoded chemical shift evolution followed by spatially resolved acquisition [7], reconstruction of multidimensional spectra from the sets of projections (projection reconstruction—PR) [8], and new variants of reduced dimensionality (RD) techniques [9,10]. Additionally, several different processing approaches designed for non-Fourier processing or interpolation of sparsely sampled multidimensional NMR data sets were proposed [11–13]. All these methods are based on the transformation of reduced quantity of data. Because signal-to-noise ratio increases with the number of acquired data points, it is obvious that it decreases in the case of sparse sampling. Therefore, this kind of methods can be used only when achievable resolution is limited only by experiment time.

The above-mentioned RD as well as PR methods are in fact founded on the idea of Accordion Spectroscopy

* Corresponding author. Fax: +48 22 822 59 96.
E-mail address: kozmin@chem.uw.edu.pl (W. Koźmiński).

1090-7807/$ - see front matter © 2006 Elsevier Inc. All rights reserved.
doi:10.1016/j.jmr.2006.02.001

[14]. Both employ the radial sampling of two or more evolution times by setting simultaneously evolution times to: $t_1 = R\sin(\phi)$ and $t_2 = R\cos(\phi)$, where R and ϕ are the radius length and angle in polar t_1/t_2 coordinates system, respectively. However, the methods differ. While in the case of the PR methods the high dimensionality spectrum is reconstructed and could be analyzed in a standard manner, the RD data sets still require evaluation of resonance frequencies from apparent peak positions in spectrum which is not always straightforward in crowded spectra, even with full quadrature, i.e., determination of sign of all involved frequencies which simplify spectrum and enables editing. The extraction of information from the RD spectra might be performed by solving of system of linear equations for each peak [9,10] or by using more complex procedures, as for example iterative frequency identification [15,16].

Conventional FT of multidimensional data sets is given by a multidimensional integral which in 2D case could be described as:

$$S(\omega_1,\omega_2) = \int_{-\infty}^{\infty} \mathrm{d}t_1 \int_{-\infty}^{\infty} \mathrm{d}t_2 f(t_1,t_2)\exp(-\mathrm{i}\omega_1 t_1) \times \exp(-\mathrm{i}\omega_2 t_2) \tag{2}$$

it is in fact realized by a sequence of one-dimensional integrals. Algorithm of discrete data processing is to calculate first integral (which corresponds to a sum in discrete case):

$$S(t_1,\omega_2) = \sum_{t_2=0}^{t_{2\max}} f(t_1,t_2)\exp(-\mathrm{i}\omega_2 t_2) \tag{3}$$

and then the second one:

$$S(\omega_1,\omega_2) = \sum_{t_1=0}^{t_{1\max}} S(t_1,\omega_2)\exp(-\mathrm{i}\omega_1 t_1). \tag{4}$$

Such procedure can be carried out with the data sampled conventionally, i.e., performed in a way allowing one separate transformation with respect to one evolution time with the second kept constant. On the other hand, the 1D transformation of radial sampled data (where t_1 is directly proportional to t_2) from the RD or PR experiment is given by Eq. (1) with only one integral, and gives a projection spectrum of sums and differences of involved frequencies. In the latter case, selection of spectra either with sums or differences of frequencies could be obtained by application of quadrature detection rules, i.e., by recording and appropriate combination of all possible sine/cosine modulated data sets [9,10].

In this communication, we propose the application of FT with respect to two or more time variables as a reliable procedure for the processing of multidimensional NMR data sets in a single step. It is more general than inverse Radon transform [17] which is limited for processing of radial sampled data sets and circumvents the difficulties associated with analyzing of reduced dimensionality spectra. Our approach to FT of multidimensional NMR data is different in two important points. First difference is the algorithm of calculating transform integral. Instead of making sequence of two summations, equivalent to transition: $f(t_1,t_2) \overset{FT_1}{\rightarrow} S_1(t_1,\omega_2) \overset{FT_2}{\rightarrow} S(\omega_1,\omega_2)$ we could calculate two integrals over time space for each pair of frequencies, i.e., real discrete cosine transform of signal $f(t_1,t_2) = \cos(\Omega_1 t_1)\cos(\Omega_2 t_2)$ is given by:

$$S(\omega_1,\omega_2) = \sum_{t_1=0}^{t_{1\max}} \sum_{t_2=0}^{t_{2\max}} f(t_1,t_2)\cos(\omega_1 t_1)\cos(\omega_2 t_2). \tag{5}$$

In other words for each pair of frequencies (ω_1,ω_2), inside of the spectral range, the product of time domain signal $f(t_1,t_2)$ and $\cos(\omega_1 t_1)\cos(\omega_2 t_2)$ should be calculated for each point of evolution time space (t_1 and t_2) and summed. Note that this is natural two-dimensional extension of a standard 1D FT, where for one ω variable summation along one evolution time is required.

In the case of single indirectly detected time domain, the standard States [18] or States-TPPI [19], procedures to obtain quadrature detection and pure absorption lineshapes, are the methods of choice. In both cases, recording of the two amplitude modulated data sets, $\cos(\Omega t_1)$ and $\sin(\Omega t_1)$, respectively, is required. However, in the case of phase modulation in t_1, which is usually obtained using gradient echo- and anti-echo coherence selection, in sensitivity-enhanced sequences [20–22] or TROSY [23,24] experiments, the amplitude modulation should be reestablished prior to Fourier transformation. The $\cos(\Omega t_1)$ and $\sin(\Omega t_1)$ amplitude modulated interferograms are calculated as the sum and difference of echo- and anti-echo data sets, respectively, followed by $\pi/2$ phase correction along the directly detected time domain. The cosine and sine modulated interferograms correspond to symmetric and antisymmetric spectra in frequency domain and are used for Fourier transform as real and imaginary parts, respectively. Consequently, in the case of any NMR experiment with N indirectly measured dimensions it is necessary to achieve 2^N differently modulated functions of evolution times. In the reduced dimensionality spectra the full quadrature and all possible frequency signs could be obtained by the linear combination of acquired data sets followed by the usual complex Fourier transform [9,10].

In the general 2D NMR experiment, according to the above-mentioned rules of quadrature detection, the four differently modulated data sets should be recorded. Their transforms could be described as:

$$f(t_1,t_2) = \cos(\Omega_1 t_1)\cos(\Omega_2 t_2) \rightarrow S(\omega_1,\omega_2) = \sum_{t_1=0}^{t_{1\max}} \sum_{t_2=0}^{t_{2\max}} f(t_1,t_2)\cos(\omega_1 t_1)\cos(\omega_2 t_2), \tag{6a}$$

$$f(t_1,t_2) = \cos(\Omega_1 t_1)\sin(\Omega_2 t_2) \rightarrow S(\omega_1,\omega_2) = \sum_{t_1=0}^{t_{1\max}} \sum_{t_2=0}^{t_{2\max}} f(t_1,t_2)\cos(\omega_1 t_1)\sin(\omega_2 t_2), \tag{6b}$$

$$f(t_1,t_2)=\sin(\Omega_1 t_1)\sin(\Omega_2 t_2)\rightarrow S(\omega_1,\omega_2)$$
$$=\sum_{t_1=0}^{t_{1\max}}\sum_{t_2=0}^{t_{2\max}} f(t_1,t_2)\sin(\omega_1 t_1)\sin(\omega_2 t_2), \tag{6c}$$
$$f(t_1,t_2)=\sin(\Omega_1 t_1)\cos(\Omega_2 t_2)\rightarrow S(\omega_1,\omega_2)$$
$$=\sum_{t_1=0}^{t_{1\max}}\sum_{t_2=0}^{t_{2\max}} f(t_1,t_2)\sin(\omega_1 t_1)\cos(\omega_2 t_2). \tag{6d}$$

In order to find exact value and sign of Ω_1 and Ω_2 frequencies, the above terms should be combined in the following way:

$$\sum_{t_1=0}^{t_{1\max}}\sum_{t_2=0}^{t_{2\max}} f(t_1,t_2)\cos(\omega_1 t_1)\cos(\omega_2 t_2)$$
$$-\sum_{t_1=0}^{t_{1\max}}\sum_{t_2=0}^{t_{2\max}} f(t_1,t_2)\cos(\omega_1 t_1)\sin(\omega_2 t_2)$$
$$+\sum_{t_1=0}^{t_{1\max}}\sum_{t_2=0}^{t_{2\max}} f(t_1,t_2)\sin(\omega_1 t_1)\sin(\omega_2 t_2)$$
$$-\sum_{t_1=0}^{t_{1\max}}\sum_{t_2=0}^{t_{2\max}} f(t_1,t_2)\sin(\omega_1 t_1)\cos(\omega_2 t_2). \tag{7}$$

The above solution is natural extension of quadrature in 1D case which is described by real part of complex FT Eq. (1). To find the form of above sum, the quaternion, rather than complex FT, should be considered, which is the second difference in comparison to established in NMR spectroscopy and imaging solutions.

Quaternions [25] are four-dimensional non-commutative extension of complex numbers (which represent 2D vector) and FT acting on them is used for example in image processing [26,27], instead of complex FT. Quaternion representation Q of vector (x_0,x_1,x_2,x_3) is:

$$Q=x_0+\mathrm{i}x_1+\mathrm{j}x_2+\mathrm{k}x_3, \tag{8}$$

where $\mathrm{i}^2=\mathrm{j}^2=\mathrm{k}^2=-1$ and $\mathrm{ij}=-\mathrm{ji}=\mathrm{k}$, $\mathrm{jk}=-\mathrm{kj}=\mathrm{i}$, and $\mathrm{ki}=-\mathrm{ik}=\mathrm{j}$.

Now neglecting relaxation terms, we could consider 2D time domain signal as:

$$f(t_1,t_2)=\exp(-\mathrm{i}\Omega_1 t_1)\exp(-\mathrm{j}\Omega_2 t_2)$$
$$=\cos(\Omega_1 t_1)\cos(\Omega_2 t_2)-\mathrm{i}\sin(\Omega_1 t_1)\cos(\Omega_2 t_2)$$
$$-\mathrm{j}\cos(\Omega_1 t_1)\sin(\Omega_2 t_2)+\mathrm{k}\sin(\Omega_1 t_1)\sin(\Omega_2 t_2). \tag{9}$$

The Quaternion FT is then given by the integral which differ from Eq. (2) by the second imaginary unit j:

$$S(\omega_1,\omega_2)=\int\int \mathrm{d}t_1\,\mathrm{d}t_2\exp(-\mathrm{i}\omega_1 t_1)f(t_1,t_2)$$
$$\times\exp(-\mathrm{j}\omega_2 t_2). \tag{10}$$

Its real part is simple to calculate, from the four standard data sets measured using the rules of quadrature detection:

$$\mathrm{Re}\,[S(\omega_1,\omega_2)]$$
$$=\int\int \mathrm{d}t_1\,\mathrm{d}t_2\cos(\Omega_1 t_1)\cos(\Omega_2 t_2)\cos(\omega_1 t_1)\cos(\omega_2 t_2)$$
$$-\int\int \mathrm{d}t_1\,\mathrm{d}t_2\cos(\Omega_1 t_1)\sin(\Omega_2 t_2)\cos(\omega_1 t_1)\sin(\omega_2 t_2)$$
$$-\int\int \mathrm{d}t_1\,\mathrm{d}t_2\sin(\Omega_1 t_1)\cos(\Omega_2 t_2)\sin(\omega_1 t_1)\cos(\omega_2 t_2)$$
$$+\int\int \mathrm{d}t_1\,\mathrm{d}t_2\sin(\Omega_1 t_1)\sin(\Omega_2 t_2)\sin(\omega_1 t_1)\sin(\omega_2 t_2). \tag{11}$$

It should be noted that this result could not be obtained from Eq. (2) applied to complex 2D NMR signal of $\exp(-\mathrm{i}\Omega_1 t_1)\exp(-\mathrm{i}\Omega_2 t_2)$.

The solution given in Eqs. (10) and (11) provides no restrictions to sampling procedure except one: there remains only the necessity to fulfill Nyquist theorem. In a 2D case the proper sampling of 2D signal in the range of sw_1 and sw_2 spectral widths requires measurements of points of evolution time space which coordinate differences (τ_1,τ_2) fulfill the condition:

$$sw_1\tau_1+sw_2\tau_2<1. \tag{12}$$

This approach to the FT is fully scalable and the addition of third sampled evolution time would simply double the number of components in Eq. (11). It would also require performing calculations for each $S(\omega_1,\omega_2,\omega_3)$ point.

We decided to apply the FT as described above for processing of the 3D HNCO spectra measured for doubly labeled ^{15}N,^{13}C-ubiquitin sample using radial and spiral sampling of t_1,t_2 space. Therefore, we employed a standard 1D FT with respect to t_3, followed by the 2D Quaternion FT with respect to t_1 and t_2 calculated for each ω_3 frequency point. We sampled data only for $0\leqslant\phi\leqslant\pi/2$ angles in polar coordinate system, since the data for negative evolution times are equivalent to inversion of the imaginary part of the respective signal. The data were collected using standard pulse sequence, modified only by setting t_2 and t_1 evolution times as defined in Eqs. (13) and (14) for the radial and spiral sampling, respectively, and incrementing R.

$$t_1=R\sin(\phi),\quad t_2=R\cos(\phi), \tag{13}$$
$$t_1=R|\sin(\phi)|,\quad t_2=R|\cos(\phi)|,\qquad \phi=aR. \tag{14}$$

In the case of spiral sampling, we doubled number of time domain data points using both possible directions, i.e., the second was obtained by reversing of t_1 and t_2. The comparison of obtained F_1F_2 planes for ω_3 (^{1}H) = 8.81 ppm is given in Fig. 1. It is clearly visible that the spectra obtained by Fourier transform of radial and spiral sampled t_1/t_2 domain data (Figs. 1B and C), respectively, give rise to proper spectra and retain the full information of conventional 3D spectrum (Fig. 1A) while the measurement time could be significantly shortened. However, as shown in Fig. 2 which compares slices with lower contour levels (for the spiral

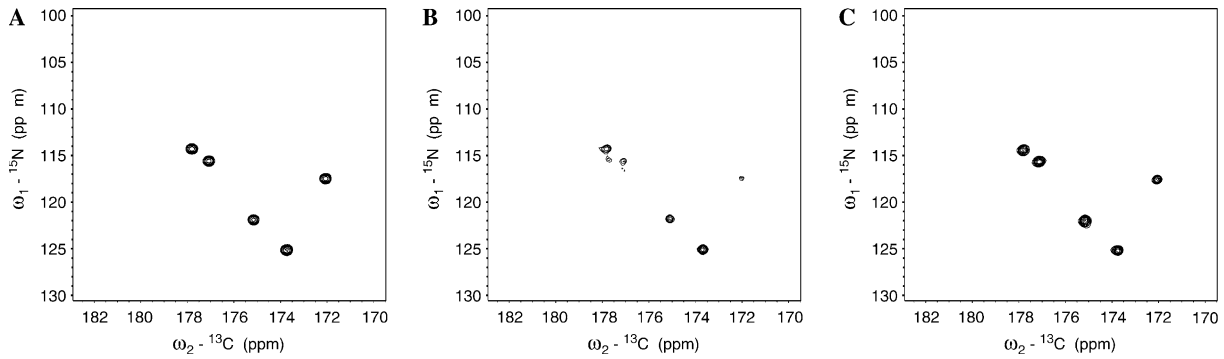

Fig. 1. Comparison of F_1/F_2 planes for $\omega_3(^1\mathrm{H}) = 8.81$ ppm. (A) Conventional HNCO; (B) radial sampled HNCO, three projection angles of 4.5°, 45°, and 85.5°; (C) spiral sampled HNCO, ϕ incremented by 40.4° in both directions for each R value, according to Eq. (11). Measurement time of 10 h 34 min (1600 t_1/t_2 data points), 1 h 35 min (240 t_1/t_2 data points), and 1 h 3 min (160 t_1/t_2 data points), for spectra presented in (A), (B), and (C), respectively.

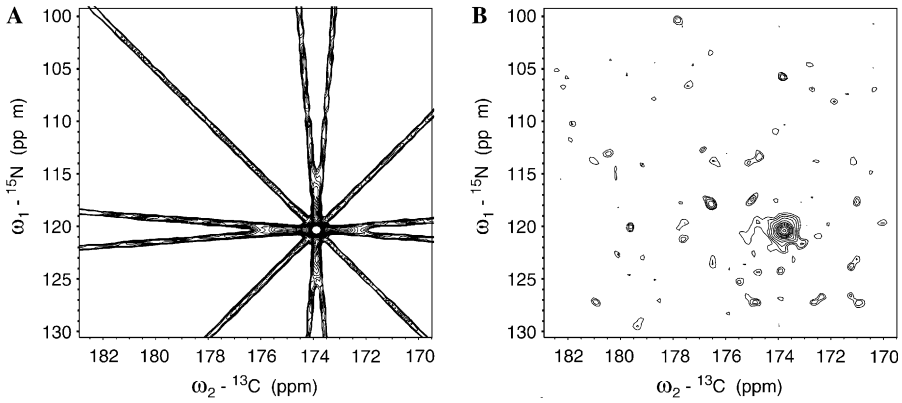

Fig. 2. Comparison of F_1/F_2 planes with increased intensity scale (A), and (B) radial and spiral sampled spectra, respectively. The scale of slice (B) is ca. fivefold larger. The plane of $\omega_3(^1\mathrm{H}) = 6.28$ ppm with single signal was chosen for clear comparison.

sampled spectrum threshold is ca. fivefold lower), Fourier transformation of radial sampled interferogram (Fig. 2A) is much more prone to artifacts than spectrum obtained from spiral data (Fig. 2B). For the clarity of comparison the slice with only one signal was chosen. The resolution achieved in all three spectra is very similar, however, the signal-to-noise ratio of spiral sampled HNCO in approximately 1 h is 4–5 times weaker than obtained for conventional 10.5 h HNCO. This result is worse than expected from comparison of the number of measured t_1/t_2 data points, i.e., $\sqrt{10}$, which might be explained by the artifacts introduced by sampling scheme.

The influence of distribution of time domain data points into appearance of artifacts in transformed spectrum is illustrated in Fig. 3. All plots are obtained using Fourier transform defined in Eq. (7), with the same number of simulated data points. The time domain data points were calculated assuming only one signal and the relaxation time equal to maximum evolution times. Figs. 3A and B are obtained using radial sampled data along 3 and 15 different lines, respectively. The results clearly indicate the artifacts analogous to those associated with Radon transform of radial sampled data. Their origin is due to the same ambiguity, but in this case for each projection two lines crossing the cross-peak are observed for which the sum of $\cos(\phi)\omega_1 \pm \sin(\phi)\omega_2$ is constant. With the increasing number of sampled lines precision of signal position and its relative intensity increases proportionally. Similarly as in the case of Radon transform it is not possible to obtain spectrum free of artifacts. The transform of spiral sampled data, excluding situation when the integer number of ϕ angle increments is equal to $\pi/2$ forming set of the lines, behaves differently. The comparison of Fourier transform using differently spiral sampled data is given in Figs. 3C and D. The obtained spectra exhibit significant differences. Although the spectrum 3c obtained from spiral data with only 1/4 of spiral turn is full of artifacts, using of the same number of points but distributed in 7 turns significantly improved the spectrum quality owing to their better dispersion in the time space. The main drawback of radial sampling is creation of false maxima on the artifact line crossings in the whole spectrum range, due to their constant intensity. Different situation is observed in transform of spiral sampled data. In this case, much less artifacts are observed and they are spread over whole spectrum with quickly lowering intensity. Thus, superposition of artifacts is much less likely.

The ideal sampling should uniformly cover the entire t_1/t_2 space with as high as possible number of data points. This is the case of conventional sampling with equispaced

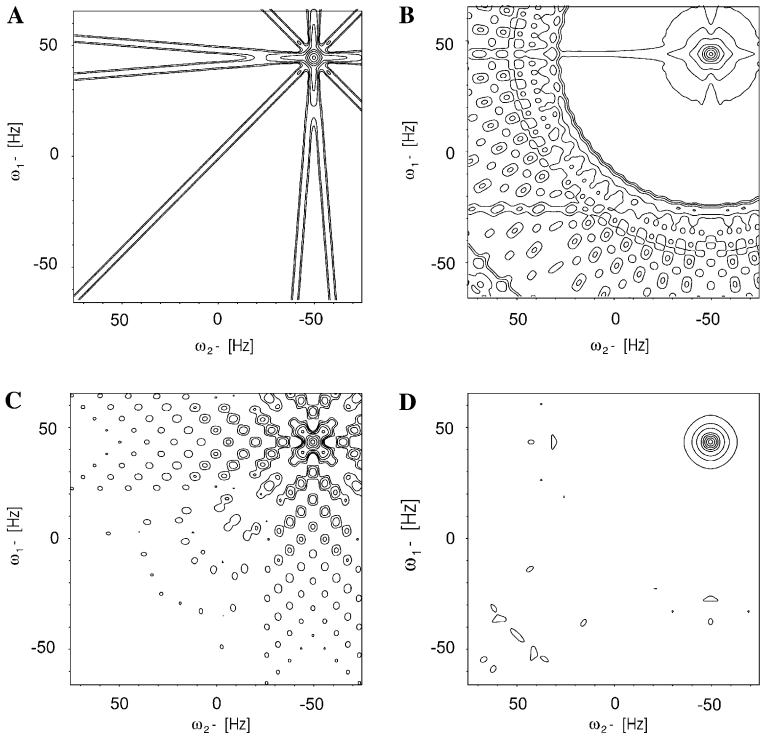

Fig. 3. Comparison of simulated 2D spectra transformed according to Eq. (7) using differently distributed time domain data points. For all spectra 256 time domain t_1/t_2 points in the range of 0–1 s were simulated using $\nu_1 = 50$ Hz, $\nu_2 = -50$ Hz. (A and B) Transformation of radial data along 3 (tilted by $\phi = 4.5°$, 45°, and 85.5°) and 15 (with ϕ incremented in 6° steps) lines, respectively. (C and D) Spectra obtained using spiral data with two spirals going in opposite directions according to Eq. (14). The maximum ϕ is equal to $\pi/2$ and 14π in spectra (C) and (D), respectively. All spectra are plotted in the same scale allowing to observe artifacts level.

time domain data points. It is noticeable that in such situation the result does not depend on the applied transformation algorithm. However, using as an input for transformation non-uniformly dispersed time domain data points generate artifacts whose intensity and appearance strongly depend on the sampling scheme. This effect attenuates obtainable signal-to-noise ratio in such experiments.

The proposed method of processing of multidimensional NMR data sets is not limited to the radial sampling used in RD and PR techniques. We demonstrated that the different sampling schemes like spiral provide much cleaner spectra due to better dispersion of data points in the evolution time space. In comparison to RD approach the new method provides NMR spectra of full dimensionality which could be analyzed directly, however, sparse sampling might introduce unwanted artifacts. The method could be useful to increase obtainable resolution in the limited experiment time.

Concluding, we shown a simple and general extension of multidimensional Fourier transform acting on more than one time variable. Such a procedure allows one to process arbitrarily sampled multidimensional NMR data significantly reducing experiment time while retaining readability and resolution of high dimensionality. We find that spiral sampling of time domain provides much cleaner data than radial sampling in comparable experiment time, however, the new sampling schemes should be optimized, and a number of other strategies, as for example differently incremented spirals or even random sampling, could also be useful. The described technique could be also applied for processing of unconventionally sampled Magnetic Resonance Imaging signals without necessity of time domain signal interpolation.

2. Experimental

All the spectra presented were recorded for 1.5 mM ^{13}C,^{15}N-labeled ubiquitin in 9:1 H_2O/D_2O at pH 4.5 at 298 K on a Varian Unity Plus 500 spectrometer equipped with a Performa II z-PFG unit and a 5 mm ^{1}H,^{13}C,^{15}N-triple resonance probehead. High power ^{1}H, ^{13}C, and ^{15}N $\pi/2$ pulses of 6.7, 14.0, and 44.0 μs, respectively, were employed. For the radial and spiral sampling the conventional HNCO sequence was adapted from the Varian Userlib ProteinPack package by setting evolution times accordingly to Eqs. (13) and (14), respectively. For all presented spectra, four scans were coherently added for four data sets for each t_1/t_2 data point, the acquisition time of 85 ms and relaxation delay of 1.4 s were used. For conventional HNCO spectrum, 40 t_1 and t_2 increments were measured for the maximum t_1 and t_2 times of 23.5 and 25 ms, respectively. In the case of radial and spiral sampling, the radius was incremented up to 24.2 ms in 80 steps. Cosine square weighting function was applied prior to Fourier transformation in both dimensions, and data are transformed for

$128 \times 128 \times 1024$ real points in F_1, F_2, and F_3, respectively. The radial and spiral sampled t_1/t_2 interferograms were transformed on PC with 3.0 GHz Pentium 4 processor under Linux operating system using C code. The computing time for radial and spiral data was 23 and 15 min, for 240 and 160 t_1/t_2 data points, respectively. The resulting real parts of 3D spectra were saved in the format of SPARKY [28] program.

References

[1] R.R. Ernst, W.A. Anderson, Application of Fourier transform spectroscopy to magnetic resonance, Rev. Sci. Instrum. 37 (1966) 93–102.

[2] T. Szyperski, D.C. Yeh, D.K. Sukumaran, H.N.B. Moseley, G.T. Montelione, Reduced-dimensionality NMR spectroscopy for high-throughput protein resonance assignment, Proc. Natl. Acad. Sci. USA 99 (2002) 8009–8014.

[3] Ē. Kupče, R. Freeman, New methods for fast multidimensional NMR, J. Biomol. NMR 27 (2003) 101–113.

[4] B. Simon, M. Sattler, Speeding up biomolecular NMR spectroscopy, Angew. Chem. Int. Ed. Engl. 43 (2004) 782–786.

[5] D. Malmodin, M. Billeter, High-throughput analysis of protein NMR spectra, Prog. Nucl. Magn. Reson. Spectrosc. 46 (2005) 109–129.

[6] R. Freeman, Ē. Kupče, Distant echoes of the accordion: reduced dimensionality, GFT-NMR, and projection-reconstruction of multidimensional spectra, Concepts Magn. Reson. A 23 (2004) 63–75.

[7] L. Frydman, T. Scherf, A. Lupulescu, The acquisition of multidimensional NMR spectra within a single scan, Proc. Natl. Acad. Sci. USA 99 (2002) 15662–15858.

[8] Ē. Kupče, R. Freeman, Projection-reconstruction of three-dimensional NMR spectra, J. Am. Chem. Soc. 125 (2003) 13958–13959.

[9] S. Kim, T. Szyperski, GFT NMR, a new approach to rapidly obtain precise high-dimensional NMR spectral information, J. Am. Chem. Soc. 125 (2003) 1385–1393.

[10] W. Koźmiński, I. Zhukov, Multiple quadrature detection in reduced dimensionality experiments, J. Biomol. NMR 26 (2003) 157–166.

[11] D. Marion, Fast acquisition of NMR spectra using Fourier transform of non-equispaced data, J. Biomol. NMR 32 (2005) 141–150.

[12] G. Amstrong, V.A. Mandelshtam, A.J. Shaka, B. Bendiak, Rapid high-resolution four-dimensional NMR spectroscopy using the filter diagonalization method and its advantages for detailed structural elucidation of oligosaccharides, J. Magn. Reson. 173 (2005) 160–168.

[13] D. Rovnyak, D.P. Frueh, M. Sastry, Z.-Y.J. Sun, A.S. Stern, J.C. Hoch, G. Wagner, Accelerated acquisition of high resolution triple-resonance spectra using non-uniform sampling and maximum entropy reconstruction, J. Magn. Reson. 170 (2004) 15–21.

[14] G. Bodenhausen, R.R. Ernst, The accordion experiment, a simple approach to three-dimensional NMR spectroscopy, J. Magn. Reson. 45 (1981) 367–373.

[15] H.R. Eghbalnia, A. Bahrami, M. Tonelli, K. Hallenga, J.L. Markley, High-resolution iterative frequency identification for NMR as a general strategy for multidimensional data collection, J. Am. Chem. Soc. 127 (2005) 12528–12536.

[16] D. Malmodin, M. Bileter, Signal identification in NMR spectra with coupled evolution periods, J. Magn. Reson. 176 (2005) 47–53.

[17] Ē. Kupče, R. Freeman, The Radon transform: a new scheme for fast multidimensional NMR, Concepts Magn. Reson. 22A (2004) 4–11.

[18] D.J. States, R.A. Haberkorn, R.J. Ruben, A two-dimensional nuclear overhauser experiment with pure absorption phase in four quadrants, J. Magn. Reson. 48 (1982) 286–292.

[19] D. Marion, M. Ikura, R. Tschudin, A. Bax, Rapid recording of 2D NMR spectra without phase cycling. Application to the study of hydrogen exchange in proteins, J. Magn. Reson. 85 (1989) 393–399.

[20] A.G. Palmer III, J. Cavanagh, P.E. Wright, M. Rance, Sensitivity improvement in proton-detected two-dimensional heteronuclear correlation NMR spectroscopy, J. Magn. Reson. 93 (1991) 151–170.

[21] L.E. Kay, P. Keifer, T. Saarinen, Pure absorption gradient enhanced heteronuclear single quantum correlation spectroscopy with improved sensitivity, J. Am. Chem. Soc. 114 (1992) 10663–10665.

[22] M. Sattler, M.G. Schwedinger, J. Schleuchter, C. Griesinger, Novel strategies for sensitivity enhancement in heteronuclear multidimensional NMR experiments employing pulsed field gradients, J. Biomol. NMR 5 (1995) 11–22.

[23] K. Pervushin, R. Riek, G. Wider, K. Wüthrich, Attenuated T2 relaxation by mutual cancellation of dipole–dipole coupling and chemical shift anisotropy indicates an avenue to NMR structures of very large biological macromolecules in solution, Proc. Natl. Acad. Sci. USA 94 (1997) 12366–12371.

[24] J. Weigelt, Single scan, sensitivity- and gradient-enhanced TROSY for multidimensional NMR experiments, J. Am. Chem. Soc. 120 (1998) 10778–10779.

[25] W.R. Hamilton, On Quaternions, Proc. R. Ir. Acad. 3 (1847) 1–16.

[26] M. Felsberg, G. Sommer, Optimized fast algorithms for the quaternionic Fourier transform, in: Computer Analysis of Images and Patterns, Lecture Notes in Computer Science, vol. 1689, 1999, pp. 209–216.

[27] T. Bülow, G. Sommer, Hypercomplex signals—a novel extension of the analytic signal to multidimensional case, IEEE Trans. Signal Process. 49 (2001) 2844–2852.

[28] T.D. Goddard, D.G. Kneller, SPARKY 3, University of California, San Francisco.